SIAM J. SCI. COMPUT.
Vol. 46, No. 4, pp. A2503–A2527

A SEMI-IMPLICIT FULLY EXACTLY WELL-BALANCED RELAXATION SCHEME FOR THE SHALLOW WATER SYSTEM*

CELIA CABALLERO-CÁRDENAS†, MANUEL JESÚS CASTRO†,
CHRISTOPHE CHALONS‡, TOMÁS MORALES DE LUNA†, AND
MARÍA LUZ MUÑOZ-RUIZ†

Abstract. This article focuses on the design of semi-implicit schemes that are fully well-balanced for the one-dimensional shallow water equations, that is, schemes that preserve all smooth steady states of the system and not just water-at-rest equilibria. The proposed methods outperform standard explicit schemes in the low-Froude regime, where the celerity is much larger than the fluid velocity, eliminating the need for a large number of iterations on large time intervals. In this work, splitting and relaxation techniques are combined in order to obtain fully well-balanced semi-implicit first and second order schemes. In contrast to recent Lagrangian-based approaches, this one allows the preservation of all the steady states while avoiding the complexities associated with Lagrangian formalism.

Key words. fully exactly well-balanced schemes, relaxation schemes, semi-implicit schemes, shallow water

MSC codes. 76M12, 35L60, 65M08

DOI. 10.1137/23M1621289

1. Introduction.

The aim of this work is the design of semi-implicit schemes that are fully well-balanced for the one-dimensional (1D) shallow water equations. By fully well-balanced we mean that the scheme preserves all the smooth steady states of the system, and not just a subset of them, usually water-at-rest equilibria. Furthermore, our scheme is exactly fully well-balanced, that is, it exactly preserves the steady states and not just a discrete approximation of them. Although the proposed method works in all regimes, it outperforms standard explicit schemes in the low-Froude regime, where the celerity is much bigger than the fluid velocity. Indeed, in small Froude number situations, the use of explicit schemes requires a large number of iterations on large time intervals due to the CFL time step restriction, while the use of a semi-implicit scheme avoids such time step restrictions.

Obtaining well-balanced schemes for shallow water equations has been a very active topic of research for some time now. See, for instance, the works [4, 36, 45, 31, 30, 7, 1, 26, 2, 9], in which water-at-rest steady states are preserved. There are also other works whose schemes preserve all the steady states, such as [35, 15, 53, 52, 5, 6, 19, 44, 46, 8].

Moreover, different techniques for the design of implicit or semi-implicit schemes for the shallow water models have been developed since [21]. These approaches include the application of finite volume methods in studies such as [9, 23, 51], a discontinuous

*Submitted to the journal's Numerical Algorithms for Scientific Computing section December 5, 2023; accepted for publication (in revised form) May 14, 2024; published electronically July 31, 2024.
https://doi.org/10.1137/23M1621289

Funding: This work was supported by project PID2022-137637NB-C21 funded by MCIN/AEI and ERDF, and by project PDC2022-133663-C21 funded by MCIN/AEI and European Union NextGenerationEU/PRTR. The work of the first author was supported by grant FPI2019/087773 funded by MCIN/AEI and ESF.

†Universidad de Málaga, Málaga, Spain (celiacaba@uma.es, mjcastro@uma.es, tmorales@uma.es, mlmunoz@uma.es).

‡Université Versailles Saint-Quentin-en-Yvelines, 78035 Versailles cedex, France (christophe.chalons@uvsq.fr).

Galerkin approach as seen in the works [28, 33, 50, 39, 48], finite difference methods as explored in Casulli's earlier work [21, 22], and hybrid strategies, as demonstrated in studies like those in [10, 16, 11]. In general, the idea consists of performing a splitting that allows one to separate the fast waves from the slow ones and of combining explicit and implicit schemes. However, to the best of our knowledge, no previous work has been presented in which a semi-implicit scheme preserves all the steady states of the 1D shallow water equations without the need to solve the nonlinearities associated with the pressure. The only nonlinearities presented in the schemes are those related with the computation of the local steady states, that are frozen at every time step and play a crucial role in the well-balanced character of the scheme, and those presented in the transport step (that are treated explicitly).

In the recent work [17], Lagrangian formalism was used in order to define semi-implicit schemes that preserve water-at-rest stationary solutions for the shallow water equations. Lagrangian formalism was also used in [18] to define an explicit first order fully well-balanced scheme, while in [43] an explicit high order well-balanced scheme was presented. Nevertheless, the use of Lagrangian formalism complicates in excess the task of defining high order, semi-implicit, and fully well-balanced schemes. Even in [18] particular care had to be taken in the projection step in order to obtain a fully well-balanced scheme, as a steady state in Eulerian coordinates is not necessarily a steady state in Lagrangian coordinates. Moreover, extending this technique to 2D cases could be cumbersome. Therefore, we propose here a different approach that overcomes these difficulties.

In what follows, we consider the 1D shallow water equations written as

$$
\begin{cases} \partial_t h + \partial_x(hu) = 0, \\ \partial_t(hu) + \partial_x\left(hu^2 + g\dfrac{h^2}{2}\right) = -gh\, z', \end{cases} \tag{1.1}
$$

where $z(x)$ is the given smooth topography, g is the gravity constant, h is the water depth, and u is the water velocity. We shall denote by $\eta = h + z$ the free surface of the flow and by $q = hu$ the discharge.

Let us recall that the shallow water system is hyperbolic over $\Omega = \{(h, hu)^T \in \mathbb{R}^2 |\, h > 0\}$, presenting two eigenvalues: $u - c$ and $u + c$, where $c = \sqrt{gh}$ stands for the sound speed or celerity. One can distinguish two regions: the subcritical (or subsonic) region, in which $u^2 < c^2$, and the supercritical (or supersonic) one, in which $u^2 > c^2$. These regions can also be characterized in terms of the Froude number, defined as $F_r = \frac{|u|}{\sqrt{gh}}$. The subcritical regions are the ones in which $F_r < 1$, while in the supercritical ones, $F_r > 1$. Here we will focus especially on applications related to the former, since this is the case where the implicit treatment of the pressure terms is particularly worthwhile in order to avoid the use of an overly restrictive CFL condition.

A special class of solutions for shallow water equations are the so-called equilibrium or steady states, which are given by

$$
\begin{cases} \dfrac{d}{dx}(hu)^e = 0, \\ \dfrac{d}{dx}\left(hu^2 + g\dfrac{h^2}{2}\right)^e = -gh^e\, z'. \end{cases} \tag{1.2}
$$

In particular, smooth equilibria satisfy

$$\begin{cases} (hu)^e = C_1, \\ \dfrac{(u^e)^2}{2} + g(h^e + z) = C_2, \end{cases} \tag{1.3}$$

where C_1 and C_2 are two real constants. When $C_1 = 0$, we obtain the so-called lake-at-rest steady states, for which

$$q^e = (hu)^e = 0, \quad \eta^e = h^e + z = cst.$$

Note that for any two fixed constants C_1 and C_2, system (1.3) is equivalent to setting $q^e(x) = C_1$ and $h^e(x)$ solution of the cubic equation

$$(h^e)^3 + \left(z - \frac{C_2}{g}\right)(h^e)^2 + \frac{C_1^2}{2g} = 0. \tag{1.4}$$

Note that (1.4) does not always has a physical solution. It always has a negative root, but it does not always have positive ones.

Moreover, for fixed values C_1 and C_2, one may define the function

$$\begin{array}{rcl} f_{C_1} : (0, \infty] & \to & \mathbb{R}, \\ h & \mapsto & \dfrac{C_1^2}{2h^2} + gh \end{array}$$

and write (1.4) equivalently as

$$f_{C_1}(h) = C_2 - gz.$$

Following the study done in [15], for any fixed value C_1, f_{C_1} has a global minimum at

$$h_{crit}(C_1) = \frac{|C_1|^{2/3}}{g^{1/3}}. \tag{1.5}$$

Let us denote by $m_s(C_1) = f_{C_1}(h_{crit}(C_1))$. Then one can find three different possibilities when solving (1.4):

1. If $C_2 - gz < m_s(C_1)$, then there exists no real positive solution.
2. It $C_2 - gz = m_s(C_1)$, then there exists a unique real positive solution given by $h = h_{crit}(C_1)$.
3. If $C_2 - gz > m_s(C_1)$, then there are exactly two positive solutions: the subcritical one that satisfies $h > h_{crit}(C_1)$ and the supercritical one that verifies $h < h_{crit}(C_1)$.

Even though in the literature we can find different definitions of well-balanced schemes, in this work we will consider the ones used in [34], so when a scheme exactly preserves the steady states it is said to be exactly well-balanced, while if it preserves a discrete approximation of them, it is called well-balanced.

We aim then to define a semi-implicit fully exactly well-balanced scheme, specially adapted for small Froude number situations. The used splitting strategy can be motivated by properly rescaling the equations. Indeed, if we consider the dimensionless form of the shallow water equations, the Froude number will appear accompanying the pressure terms, in such a way that their relevance increases as the Froude number decreases [25, 32]. The splitting strategy introduced in [37] for the Euler compressible system and developed in [29] for the Ripa equations will be combined with a relaxation technique and will be described in section 2, where we will also be concerned with the design of schemes that are well-balanced. In sections 3 and 4, the proposed first and second order schemes are presented, respectively. Finally, several numerical experiments are shown in section 5 in order to test the accuracy and efficiency of the schemes presented.

2. Splitting and relaxation techniques. We will start by proposing a relaxed system for (1.1), making use of relaxation techniques following the ideas of [38, 27, 3, 12, 24, 14, 49]. The proposed relaxed system is given by

$$\begin{cases} \partial_t h + \partial_x (hu) = 0, \\ \partial_t (hu) + \partial_x (hu^2 + \pi) = -gh\, z', \\ \partial_t (h\pi) + a^2 \partial_x u = \dfrac{1}{\varepsilon}\left(\dfrac{1}{2} g h^2 - \pi\right), \end{cases} \tag{2.1}$$

where a is a constant satisfying the subcharacteristic condition, that is, following [13], one should have

$$a \geq h\sqrt{gh}. \tag{2.2}$$

Note that in the limit case $\varepsilon \to 0$ we have $\pi = \frac{1}{2}gh^2$. Therefore, the ε-source term in (2.1) is usually neglected and then π is initialized to the pressure $\frac{1}{2}gh^2$ at each time step.

We will now perform a splitting of system (2.1). In order to set the basic ideas that will be detailed afterward, let us rewrite the system as

$$\partial_t U = S_P(U, z) + S_T(U),$$

where $U = (h, hu, h\pi)^T$,

$$S_P(U, z) = \begin{bmatrix} 0 \\ -\partial_x \pi - gh\, z' \\ -a^2 \partial_x u \end{bmatrix}, \tag{2.3}$$

and

$$S_T(U) = \begin{bmatrix} -\partial_x (hu) \\ -\partial_x (hu^2) \\ 0 \end{bmatrix}. \tag{2.4}$$

The splitting strategy consists in solving each of the two systems

$$\partial_t U = S_P(U, z) \tag{2.5}$$

and

$$\partial_t U = S_T(U) \tag{2.6}$$

sequentially.

System (2.5) will be referred to as the pressure system, while system (2.6) will be referred to as the transport system.

We could either solve the system defined by S_P first, followed by the one defined by S_T, or vice versa.

The advantage of applying this splitting approach is that it decouples the acoustic and the transport phenomena. This way, the pressure system can be solved both explicitly or implicitly, while the transport system will always be solved explicitly. Performing the pressure step implicitly allows us to consider larger time steps since it involves a less restrictive CFL condition. Indeed, for small Froude numbers, the main restriction on the time step is driven by the pressure term. The reason why this happens is that system (2.5) has eigenvalues

$$\lambda = 0 \text{ and } \lambda = \pm\frac{a}{h}, \tag{2.7}$$

while system (2.6) has eigenvalues given by

$$\lambda = u \text{ (double) and } \lambda = 0. \tag{2.8}$$

Let us now describe in detail how each of the systems will be solved. First, we consider the general framework of finite volume schemes: the computational domain is discretized in a set of cells $[x_{i-1/2}, x_{i+1/2})$ for $i \in \mathbb{Z}$ using, for the sake of simplicity, a constant volume length $\Delta x = x_{i+1/2} - x_{i-1/2}$. The values $x_{i+1/2}$ correspond to the intercells, while the centers of the volume cells will be denoted by $x_i = (x_{i-1/2} + x_{i+1/2})/2$. The time variable will be kept continuous for now and the approximation of the cell averages will be denoted by

$$(h_i(t), (hu)_i(t), (h\pi)_i(t))^T = U_i(t) \approx \frac{1}{\Delta x}\int_{x_{i-1/2}}^{x_{i+1/2}} U(x,t)dx.$$

A semidiscrete finite volume scheme for systems (2.5)–(2.6) can be written as

$$\begin{cases} h_i'(t) = 0, \\ (hu)_i'(t) = -\frac{1}{\Delta x}\left(\pi^*_{i+1/2}(t) - \pi^*_{i-1/2}(t)\right) + S_i(t), \\ (h\pi)_i'(t) = -\frac{a^2}{\Delta x}\left(u^*_{i+1/2}(t) - u^*_{i-1/2}(t)\right), \end{cases} \tag{2.9}$$

$$\begin{cases} h_i'(t) = -\frac{1}{\Delta x}\left(h^*_{i+1/2}(t)u^*_{i+1/2}(t) - h^*_{i-1/2}(t)u^*_{i-1/2}(t)\right), \\ (hu)_i'(t) = -\frac{1}{\Delta x}\left((hu)^*_{i+1/2}(t)u^*_{i+1/2}(t) - (hu)^*_{i-1/2}(t)u^*_{i-1/2}(t)\right), \\ (h\pi)_i'(t) = 0, \end{cases} \tag{2.10}$$

or in compact form as

$$\frac{d}{dt}U_i(t) = S_{P\,i}(t), \tag{2.11}$$

$$\frac{d}{dt}U_i(t) = S_{T\,i}(t), \tag{2.12}$$

where

$$S_{P\,i}(t) = \begin{pmatrix} 0 \\ -\frac{1}{\Delta x}\left(\pi^*_{i+1/2}(t) - \pi^*_{i-1/2}(t)\right) + S_i(t) \\ -\frac{a^2}{\Delta x}\left(u^*_{i+1/2}(t) - u^*_{i-1/2}(t)\right) \end{pmatrix},$$

$$S_{P\,i}(t) = \begin{pmatrix} -\frac{1}{\Delta x}\left(h^*_{i+1/2}(t)u^*_{i+1/2}(t) - h^*_{i-1/2}(t)u^*_{i-1/2}(t)\right) \\ -\frac{1}{\Delta x}\left((hu)^*_{i+1/2}(t)u^*_{i+1/2}(t) - (hu)^*_{i-1/2}(t)u^*_{i-1/2}(t)\right) \\ 0 \end{pmatrix}.$$

The notation with the asterisk is usually employed in the field of Lagrange-projection schemes, so it will be used here for continuity with previous work.

Here, $h^*_{i\pm1/2}(t)$ and $(hu)^*_{i\pm1/2}(t)$ are approximations at the interface of the height and the discharge, that is, $h^*_{i+1/2}(t) \approx h(x_{i\pm\frac{1}{2}}, t)$ and $h^*_{i+1/2}(t) \approx (hu)(x_{i\pm\frac{1}{2}}, t)$, while $\pi^*_{i\pm\frac{1}{2}}(t)$ and $u^*_{i\pm\frac{1}{2}}(t)$ are approximations at the interface of the pressure $\pi = \frac{g}{2}h^2$ and the velocity u, respectively: $\pi^*_{i\pm\frac{1}{2}}(t) \approx \pi(x_{i\pm\frac{1}{2}}, t)$ and $u^*_{i\pm\frac{1}{2}}(t) \approx u(x_{i\pm\frac{1}{2}}, t)$. Note that $\pi^*_{i\pm1/2}$, $u^*_{i\pm1/2}$, $h^*_{i\pm1/2}$, and $(hu)^*_{i\pm1/2}$ could be seen as numerical fluxes. The approximation of the source term is denoted by $S_i(t)$, that is,

$$S_i(t) \approx \frac{1}{\Delta x}\int_{x_{i-1/2}}^{x_{i+1/2}} gh(x,t)z'(x)dx.$$

Now, in view of system (2.9), as h_i is constant through time, h_i is frozen at $t = t_0$. In practice it will be frozen at the corresponding time step, every time the pressure system is solved. Now, if first and second order finite volume schemes are considered and focusing on the equations for u and π, we could write (2.9) as follows:

$$\begin{cases} u_i'(t) = -\dfrac{1}{h_i(t_0)\Delta x}\left(\pi^*_{i+1/2}(t) - \pi^*_{i-1/2}(t)\right) - \dfrac{1}{h_i(t_0)}S_i(t), \\ \pi_i'(t) = -\dfrac{a^2}{h_i(t_0)\Delta x}\left(u^*_{i+1/2}(t) - u^*_{i-1/2}(t)\right), \end{cases} \tag{2.13}$$

where $S_i(t)$ is now such that

$$S_i(t) \approx \frac{1}{\Delta x}\int_{x_{i-1/2}}^{x_{i+1/2}} gP_{i,h}(t,x)z'(x)dx,$$

with $P_{i,h}$ a reconstruction operator within the cell i for the variable $h(t,x)$.

A reconstruction operator is an operator that, given a sequence of cell averages $\{U_i\}$, provides at every cell $[x_{i-1/2}, x_{i+1/2})$ a smooth function that depends on the values at some neighbor cells whose indexes belong to the so-called stencil $\mathcal{S}_i$, that is, $P_i(x) = P_i(x, \{U_j\}_{j\in\mathcal{S}_i})$.

As h does not change in time in this step, $S_i(t)$ is no longer time dependent, so we could consider

$$S_i \approx \frac{1}{\Delta x}\int_{x_{i-1/2}}^{x_{i+1/2}} gP_{i,h_0}(x)z'(x)dx,$$

where $P_{i,h_0}(x)$ is a reconstruction of $h|_{t=t_0}(x)$, to be determined.

In practice, (2.13) can be rewritten in terms of the Riemann invariants $\overrightarrow{w} = \pi + au$ and $\overleftarrow{w} = \pi - au$ as follows:

$$\begin{cases} \overrightarrow{w}'_i(t) = -\dfrac{a}{h_i(t_0)\Delta x}\left(\overrightarrow{w}_{i+1/2}(t) - \overrightarrow{w}_{i-1/2}(t)\right) - \dfrac{a}{h_i(t_0)}S_i, \\ \overleftarrow{w}'_i(t) = \dfrac{a}{h_i(t_0)\Delta x}\left(\overleftarrow{w}_{i+1/2}(t) - \overleftarrow{w}_{i-1/2}(t)\right) + \dfrac{a}{h_i(t_0)}S_i. \end{cases} \tag{2.14}$$

Here, the approximations at the intercells $\overrightarrow{w}_{i+1/2}(t) \approx \overrightarrow{w}(x_{i+1/2}, t)$ and $\overleftarrow{w}_{i+1/2}(t) \approx \overleftarrow{w}(x_{i+1/2}, t)$, that correspond to the numerical fluxes at the intercells, will be computed using a reconstruction operator. The advantage of using the Riemann invariants is that we manage to decouple the two equations, obtaining thus two transport equations with source terms.

Note that π and u can be easily recovered from the values of $\overrightarrow{w}$ and $\overleftarrow{w}$ as follows:

$$\pi = \frac{\overrightarrow{w} + \overleftarrow{w}}{2}, \quad u = \frac{\overrightarrow{w} - \overleftarrow{w}}{2a}.$$

Therefore, once we have solved (2.14), we can make use of the previous relations and then define $\pi^*_{i+1/2}(t)$ and $u^*_{i+1/2}(t)$ as

$$\pi^*_{i+1/2}(t) = \frac{P_{i,\overrightarrow{w}}(x_{i+1/2},t) + P_{i+1,\overleftarrow{w}}(x_{i+1/2},t)}{2}, \tag{2.15}$$

$$u^*_{i+1/2}(t) = \frac{P_{i,\overrightarrow{w}}(x_{i+1/2},t) - P_{i+1,\overleftarrow{w}}(x_{i+1/2},t)}{2a}, \tag{2.16}$$

where $P_{i,\overrightarrow{w}}$ and $P_{i,\overleftarrow{w}}$ correspond to some reconstruction operators within the cell. Using (2.15)–(2.16), we can compute the values $\pi^*_{i+1/2}(t)$ and $u^*_{i+1/2}(t)$ in (2.9) and (2.10).

Once the pressure system is approximated, we will use an upwind scheme in order to solve the transport ODE system defined in (2.10). That is, the values $h^*_{i+1/2}(t)$ and $(hu)^*_{i+1/2}(t)$ are defined as

$$h^*_{i+1/2}(t) = \begin{cases} P_{h,i}(x_{i+1/2},t) \text{ if } u^*_{i+1/2}(t) \geq 0, \\ P_{h,i+1}(x_{i+1/2},t) \text{ if } u^*_{i+1/2}(t) < 0, \end{cases}$$

and

$$(hu)^*_{i+1/2}(t) = \begin{cases} P_{hu,i}(x_{i+1/2},t) \text{ if } u^*_{i+1/2}(t) \geq 0, \\ P_{hu,i+1}(x_{i+1/2},t) \text{ if } u^*_{i+1/2}(t) < 0, \end{cases}$$

where $P_{h,i}$ and $P_{hu,i}$ denote the reconstruction operator corresponding to the height and the discharge, respectively.

Although up to now the time variable has been kept continuous, the time steps will be solved afterward by means of an explicit or implicit scheme. In practice, the transport system will always be solved explicitly. Note that, for the sake of simplicity, we have not dealt yet with the well-balancing issue.

In order to achieve the exactly well-balanced character of the scheme we will follow the ideas described in [20], where the main ingredients are a fully exactly well-balanced reconstruction operator, a quadrature formula, and a proper approximation of the source term S_i that guarantees the exactly well-balanced of the numerical scheme. We recall that a fully exactly well-balanced reconstruction operator $P_i(x)$ is a reconstruction operator that satisfies

$$P_i(x, \{U^e_j\}_{j\in\mathcal{S}_i}) = U^e(x) \ \forall x \in [x_{i-1/2}, x_{i+1/2}], \ \forall i,$$

for a given continuous stationary solution U^e. We will describe our choices for the first and second order exactly well-balanced reconstruction operators in section 2.1. As we are interested in first and second order numerical schemes, we will use the midpoint rule as the quadrature formula. Therefore, we shall identify cell averages with centered point values, which is true up to second order. Finally, the approximation of the source term S_i is also done following the ideas described in [20].

More precisely, at every time step, whose initial time we denote by $t = t_0$, and at every cell, we compute the steady state $(h_i^{e,t_0}, u_i^{e,t_0})$ that satisfies (1.2) such that $h_i^{e,t_0}(x_i) = h_i^{t_0}$ and $u_i^{e,t_0}(x_i) = u_i^{t_0}$, or equivalently, the solution of (1.3) with $C_{1,i}^{t_0} = (hu)_i^{t_0}$ and

$$C_{2,i}^{t_0} = \frac{(u_i^{t_0})^2}{2} + g\left(gh_i^{t_0} + z(x_i)\right).$$

Now, integrating (1.2) over the cell $[x_{i-1/2}, x_{i+1/2}]$ we have that

$$\begin{aligned}\frac{1}{\Delta x}\int_{x_{i-1/2}}^{x_{i+1/2}} g h_i^{e,t_0}(x) z'(x)\,dx \\ = \frac{1}{\Delta x}\left(\pi_i^{e,t_0}(x_{i+1/2}) - \pi_i^{e,t_0}(x_{i-1/2}) + (hu)_i^{e,t_0}\left(u_i^{e,t_0}(x_{i+1/2}) - u_i^{e,t_0}(x_{i-1/2})\right)\right),\end{aligned}$$

where $\pi_i^{e,t_0}(x) = \frac{g}{2}(h_i^{e,t_0})^2(x)$. Taking into account the splitting procedure that we consider here, we suggest to split also this formula in the same way so that we could also rewrite systems (2.9) and (2.10) as

$$(2.17)\qquad \begin{cases} h_i'(t) &= 0, \\ (hu)_i'(t) &= -\dfrac{1}{\Delta x}\left(\pi^*_{i+1/2}(t) - \pi^*_{i-1/2}(t) - \pi_i^{e,t_0}(x_{i+1/2}) + \pi_i^{e,t_0}(x_{i-1/2})\right) \\ & \qquad -\dfrac{1}{\Delta x}\displaystyle\int_{x_{i-1/2}}^{x_{i+1/2}} g(P_{i,h_0}(x) - h_i^{e,t_0}(x)) z'(x) dx, \\ (h\pi)_i'(t) &= -\dfrac{a^2}{\Delta x}\left(u^*_{i+1/2}(t) - u^*_{i-1/2}(t)\right), \end{cases}$$

and

$$(2.18)\qquad \begin{cases} h_i'(t) = -\dfrac{1}{\Delta x}\left(h^*_{i+1/2}(t)u^*_{i+1/2}(t) - h^*_{i-1/2}(t)u^*_{i-1/2}(t)\right), \\ (hu)_i'(t) = -\dfrac{1}{\Delta x}\left((hu)^*_{i+1/2}(t)u^*_{i+1/2}(t) - (hu)^*_{i-1/2}(t)u^*_{i-1/2}(t)\right) \\ +\dfrac{1}{\Delta x}\left((hu)_i^{e,t_0}(u_i^{e,t_0}(x_{i+1/2}) - u_i^{e,t_0}(x_{i-1/2}))\right), \\ (h\pi)_i'(t) = 0. \end{cases}$$

However, given the previous semidiscrete systems, if we considered a steady state initial condition, the third equation in (2.17) would not guarantee obtaining $(h\pi)_i'(t) = 0$. The way to deal with this issue is to consider a modified relaxed system that could be seen as the relaxed system of the fluctuations:

$$(2.19)\qquad \begin{cases} \partial_t h + \partial_x(hu) = 0, \\ \partial_t(hu) + \partial_x\left(hu^2 - (hu^2)^e\right) + \partial_x\left(\pi - \pi^e\right) = -g\left(h - h^e\right) z', \\ \partial_t(h\pi) + a^2\partial_x\left(u - u^e\right) = \dfrac{1}{\varepsilon}\left(\dfrac{1}{2}gh^2 - \pi\right). \end{cases}$$

Now, applying the splitting we obtain

$$\begin{cases} h_i'(t) = 0, \\ (hu)_i'(t) = -\dfrac{1}{\Delta x}\left(\pi^*_{i+1/2}(t) - \pi^*_{i-1/2}(t) - \pi_i^{e,t_0}(x_{i+1/2}) + \pi_i^{e,t_0}(x_{i-1/2})\right) \\ \qquad\qquad -\dfrac{1}{\Delta x}\displaystyle\int_{x_{i-1/2}}^{x_{i+1/2}} g(P_{i,h_0}(x) - h_i^{e,t_0}(x))z'(x)dx, \\ (h\pi)_i'(t) = -\dfrac{a^2}{\Delta x}\left(u^*_{i+1/2}(t) - u^*_{i-1/2}(t) - u_i^{e,t_0}(x_{i+1/2}) + u_i^{e,t_0}(x_{i-1/2})\right), \end{cases} \tag{2.20}$$

and (2.18).

System (2.20) can be written analogously in terms of the Riemann invariants:

$$\begin{cases} \overrightarrow{w}_i'(t) = -\dfrac{a}{h_i(t_0)\Delta x}\left(\overrightarrow{w}_{i+1/2}(t) - \overrightarrow{w}_{i-1/2}(t) - \overrightarrow{w}_i^{e,t_0}(x_{i+1/2}) + \overrightarrow{w}_i^{e,t_0}(x_{i-1/2})\right) \\ \qquad\qquad -\dfrac{a}{h_i(t_0)\Delta x}\displaystyle\int_{x_{i-1/2}}^{x_{i+1/2}} g(P_{i,h_0}(x) - h_i^{e,t_0}(x))z'(x)dx, \\ \overleftarrow{w}_i'(t) = \dfrac{a}{h_i(t_0)\Delta x}\left(\overleftarrow{w}_{i+1/2}(t) - \overleftarrow{w}_{i-1/2}(t) - \overleftarrow{w}_i^{e,t_0}(x_{i+1/2}) + \overleftarrow{w}_i^{e,t_0}(x_{i-1/2})\right) \\ \qquad\qquad +\dfrac{a}{h_i(t_0)\Delta x}\displaystyle\int_{x_{i-1/2}}^{x_{i+1/2}} g(P_{i,h_0}(x) - h_i^{e,t_0}(x))z'(x)dx. \end{cases} \tag{2.21}$$

However, since we are considering schemes up to second order, we may apply the midpoint rule and considering that the averages correspond to the values at the center of the cells. Therefore, the source terms in (2.20) and (2.21) vanish, giving systems

$$\begin{cases} h_i'(t) = 0, \\ (hu)_i'(t) = -\dfrac{1}{\Delta x}\left(\pi^*_{i+1/2}(t) - \pi^*_{i-1/2}(t) - \pi_i^{e,t_0}(x_{i+1/2}) + \pi_i^{e,t_0}(x_{i-1/2})\right), \\ (h\pi)_i'(t) = -\dfrac{a^2}{\Delta x}\left(u^*_{i+1/2}(t) - u^*_{i-1/2}(t) - u_i^{e,t_0}(x_{i+1/2}) + u_i^{e,t_0}(x_{i-1/2})\right), \end{cases} \tag{2.22}$$

and

$$\begin{cases} \overrightarrow{w}_i'(t) = -\dfrac{a}{h_i(t_0)\Delta x}\left(\overrightarrow{w}_{i+1/2}(t) - \overrightarrow{w}_{i-1/2}(t) - \overrightarrow{w}_i^{e,t_0}(x_{i+1/2}) + \overrightarrow{w}_i^{e,t_0}(x_{i-1/2})\right), \\ \overleftarrow{w}_i'(t) = \dfrac{a}{h_i(t_0)\Delta x}\left(\overleftarrow{w}_{i+1/2}(t) - \overleftarrow{w}_{i-1/2}(t) - \overleftarrow{w}_i^{e,t_0}(x_{i+1/2}) + \overleftarrow{w}_i^{e,t_0}(x_{i-1/2})\right). \end{cases} \tag{2.23}$$

2.1. Well-balanced variable reconstructions. Let us now focus on the reconstruction of our variables. To do so, we need to keep in mind the well-balanced property and to adapt the general strategy presented in [20], combined with the ideas introduced in [17]. We recall that the algorithm proposed in [20] to construct an exact fully well-balanced reconstruction operator consists of, given a family of cell values $\{U_i\}$, at every cell $I_i = [x_{i-1/2}, x_{i+1/2})$ as follows:

1. Find, if possible, a stationary solution $U_i^{t,e}(x)$ in the cells belonging to the stencil of I_i, $\mathcal{S}_i$ such that

$$\frac{1}{\Delta x}\int_{x_{i-1/2}}^{x_{i+1/2}} U_i^{t,e}(x)\,dx = U_i(t).$$

Otherwise, take $U_i^{t,e} \equiv 0$.

Note that although the stationary solutions do not depend on time, the computed steady state is not necessarily always the same, hence the notation $U_i^{t,e}$.

2. Compute the fluctuations $\{V_j\}_{j\in S_i}$, given by

$$V_j(t) = U_j(t) - \frac{1}{\Delta x}\int_{x_{j-1/2}}^{x_{j+1/2}} U_i^{t,e}(x)\,dx, \quad j \in \mathcal{S}_i,$$

and apply a standard reconstruction operator of order p, denoted by Q, to the fluctuations:

$$Q_i^t(x) = Q_i(x; \{V_j(t)\}_{j\in\mathcal{S}_i}).$$

3. Finally, define the well-balanced reconstruction operator as

$$P_i^t(x) = U_i^{t,e}(x) + Q_i^t(x). \tag{2.24}$$

Note that in practice a quadrature formula will be used. As only first and second order reconstruction operators are considered here, the integrals are approximated by the midpoint rule.

We will now show how the reconstruction of variables is done, given in a general form for a variable X that can be either $\overrightarrow{w}$, $\overleftarrow{w}$, h, or q.

Following [17], the idea is to write the reconstruction operator at time $t \in [t_0, t_0 + \Delta t]$ as the sum of the well-balanced reconstruction operator at time t_0 and a standard reconstruction operator of the time fluctuations, that is, for any variable X we define the reconstruction operator as

$$\begin{aligned} P_{i,X}(x,t) &= P_{i,X}^{t_0}(x) + \widetilde{Q}_{i,X}(x,t) \\ &= X_i^{t_0,e}(x) + Q_{i,X}^{t_0}(x) + \widetilde{Q}_{i,X}(x,t), \quad t \in [t_0, t_0+\Delta t],\ x \in I_i, \end{aligned}$$

where $P_{i,X}^{t_0}$ and $Q_{i,X}^{t_0}$ are the reconstruction operators defined in (2.24) for variable X at time t_0, $X_i^{t_0,e}(x)$ corresponds to the value of variable X for the selected stationary state $U_i^{t_0,e}(x)$ in the cell I_i, and $\widetilde{Q}_{i,X}(x,t)$ is a reconstruction operator defined in terms of the time fluctuations, that is,

$$\widetilde{Q}_{i,X}(x,t) = \widetilde{Q}_i(x; \{X_j^{t,f}\}_{j\in\mathcal{S}_i}), \text{ where } X_j^{t,f} = X_j(t) - X_j^{t_0},\ j \in \mathcal{S}_i.$$

Note that the stationary solutions are computed at every time step at the initial time t_0.

First order reconstruction. In the first order case, the reconstruction operators $Q_{i,X}(x)$ and $\widetilde{Q}_{i,X}(x,t)$ are considered to be

$$\begin{aligned} Q_{i,X}^{t_0}(x) &= X_i^{t_0} - X_i^{e,t_0}(x_i), \\ \widetilde{Q}_{i,X}(x,t) &= X_i(t) - X_i^{t_0}. \end{aligned}$$

Therefore, the first order exactly well-balanced reconstruction operator can be written as

$$P_{i,X}^{o1}(x,t) = X_i^{e,t_0}(x) + X_i(t) - X_i^{e,t_0}(x_i). \tag{2.25}$$

Note that $\widetilde{Q}_{i,X}(x,t)$ is constant in space.

Second order reconstruction. For the second order schemes we consider

$$\begin{aligned} Q_{i,X}^{t_0}(x) &= X_i^{t_0} - X_i^{e,t_0}(x_i) + \Delta X_i^{t_0,f}(x - x_i), \\ \widetilde{Q}_{i,X}(x,t) &= X_i(t) - X_i^{t_0} + \Delta X_i^{t,f}(x - x_i). \end{aligned}$$

Hence, the exactly well-balanced reconstruction operator in this case is the following:

$$P_{i,X}^{o2}(x,t) = X_i^{e,t_0}(x) - X_i^{e,t_0}(x_i) + \Delta X_i^{t_0,f}(x - x_i) + X_i(t) + \Delta X_i^{t,f}(x - x_i). \tag{2.26}$$

Here, using the avg or harmod function limiter [42], we define

$$\Delta X_i^{t_0,f} = \frac{1}{\Delta x}\left(\phi_{i+}^{t_0}(X_i^{t_0,f} - X_{i-1}^{t_0,f}) + \phi_{i-}^{t_0}(X_{i+1}^{t_0,f} - X_i^{t_0,f})\right)$$

with

$$\phi_{i-}^{t_0} = \begin{cases} \dfrac{|d_{i-}|}{|d_{i-}| + |d_{i+}|} & \text{if } |d_{i-}| + |d_{i+}| > 0, \\ 0 & \text{otherwise,} \end{cases}$$

and

$$\phi_{i+}^{t_0} = \begin{cases} \dfrac{|d_{i+}|}{|d_{i-}| + |d_{i+}|} & \text{if } |d_{i-}| + |d_{i+}| > 0, \\ 0 & \text{otherwise,} \end{cases}$$

where $d_{i-} = X_i^{t_0,f} - X_{i-1}^{t_0,f}$ and $d_{i+} = X_{i+1}^{t_0,f} - X_i^{t_0,f}$, where

$$X_j^{t_0,f} = X_j^{t_0} - X_i^{e,t_0}(x_j)$$

for a given cell i.

Moreover,

$$\Delta X_i^{t,f} = \frac{1}{\Delta x}\left(\tilde{\phi}_{i+}^{t_0}(X_i^{t,f} - X_{i-1}^{t,f}) + \tilde{\phi}_{i-}^{t_0}(X_{i+1}^{t,f} - X_i^{t,f})\right)$$

with $\tilde{\phi}_{i\pm}^{t_0} = \phi_{i\pm}^{t_0}$ and $X_i^{t,f} = X_i(t) - X_i^{t_0}$. Note that both $\Delta X_i^{t_0,f}$ and $\Delta X_i^{t,f}$ use the same limiters computed at time t_0 to avoid nonlinearities.

THEOREM 2.1. *The schemes that result after considering the semidiscrete schemes* (2.22), (2.23), (2.18) *and the previous reconstructions* (2.25) *and* (2.26) *are fully well-balanced.*

Proof. Let us suppose that the initial condition is stationary. Then, in the first order case

$$\begin{aligned} \overrightarrow{w}_{i+1/2}(t) &= P_{i,\overrightarrow{w}}(x_{i+1/2}, t) \\ &= \overrightarrow{w}_i(t) - \pi_i^{e,t_0}(x_i) - au_i^{e,t_0}(x_i) + \pi_i^{e,t_0}(x_{i+1/2}) + au_i^{e,t_0}(x_{i+1/2}) \\ &= \overrightarrow{w}_i^{e,t_0}(x_i) - \pi_i^{e,t_0}(x_i) - au_i^{e,t_0}(x_i) + \pi_i^{e,t_0}(x_{i+1/2}) + au_i^{e,t_0}(x_{i+1/2}) \\ &= \pi_i^{e,t_0}(x_{i+1/2}) + au_i^{e,t_0}(x_{i+1/2}) = \overrightarrow{w}_i^{e,t_0}(x_{i+1/2}), \end{aligned}$$

where in the second line we are considering that the averages correspond to the values at the center of the cells. The same result holds for the other variables as well as for the second order case, since $\Delta \overrightarrow{w}_i^{t_0,f} = 0$ and $\Delta \overrightarrow{w}_i^{t,f} = 0$. The same would happen with the reconstruction of $\overleftarrow{w}$, h, and q.

Then, from (2.23) we obtain

$$\begin{cases} \overrightarrow{w}_i'(t) &= 0, \\ \overleftarrow{w}_i'(t) &= 0, \end{cases}$$

and therefore, the pressure and transport semidiscrete systems (2.22) and (2.18) are trivial, being both

$$\begin{cases} h_i'(t) = 0, \\ (hu)_i'(t) = 0, \end{cases}$$

since $\pi^*_{i\pm1/2}(t) = \pi_i^{e,t_0}(x_{i\pm1/2})$, $u^*_{i\pm1/2}(t) = u_i^{e,t_0}(x_{i\pm1/2})$, $h^*_{i\pm1/2}(t) = h_i^{e,t_0}(x_{i\pm1/2})$, $(hu)^*_{i\pm1/2}(t) = (hu)_i^{e,t_0}(x_{i\pm1/2})$. Moreover, $(hu)^*_{i\pm1/2}(t) = (hu)_i^{e,t_0}$ since the discharge at the equilibrium is constant within the ith cell.

Therefore, the stationary solution is preserved. ∎

3. First order scheme.

In this section we shall describe an exactly fully well-balanced first order scheme. Two approaches will be considered: an explicit version, where both (2.5) and (2.6) are solved explicitly, and a semi-implicit approach, where (2.5) is solved implicitly. As said previously, the semi-implicit scheme will allow us to have a less restrictive CFL condition in subcritical regimes where velocity terms are smaller than the pressure terms.

The time-stepping will be done as follows. Given a set of cell averages at time t^n, U_i^n, we solve first system (2.5) in the time interval $[t^n, t^{n+1}]$ obtaining the cell averages at time t^{n+1} and denoted by superindex $n+1-$. Then, starting from these cell averages, we solve system (2.6) in the time interval $[t^n, t^{n+1}]$, obtaining the approximation of the solution at the next time step, t^{n+1}, denoted by superindex $n+1$.

The stationary solutions will be computed as discussed in the introduction (see (1.4)), by computing the constants C_1 and C_2 with the values at the center of the cells, which in this case correspond to the averages.

3.1. Explicit scheme.

In view of the semidiscrete scheme (2.22), we propose the following first order explicit scheme for the pressure system:

$$\begin{aligned} h_i^{n+1-} &= h_i^n, \\ (hu)_i^{n+1-} &= (hu)_i^n - \frac{\Delta t}{\Delta x}\left(\pi^{*,n}_{i+1/2} - \pi^{*,n}_{i-1/2} - \pi_i^{e,n}(x_{i+1/2}) + \pi_i^{e,n}(x_{i-1/2})\right), \end{aligned} \tag{3.1}$$

where the values $\pi^{*,n}_{i+1/2}$ are computed by means of a fully well-balanced reconstruction operator for $\overrightarrow{w}$ and $\overleftarrow{w}$, given by (2.25). That is,

$$\pi^{*,n}_{i+1/2} = \frac{P^{o1}_{i,\overrightarrow{w}}(x_{i+1/2}, t^n) + P^{o1}_{i+1,\overleftarrow{w}}(x_{i+1/2}, t^n)}{2}.$$

Then, the transport system (2.18) is solved using $(h_i^{n+1-}, (hu)_i^{n+1-})$ as the initial condition:

$$\begin{aligned} h_i^{n+1} &= h_i^{n+1-} - \frac{\Delta t}{\Delta x}\left(h^{*,n+1-}_{i+1/2} u^{*,n+1-}_{i+1/2} - h^{*,n+1-}_{i-1/2} u^{*,n+1-}_{i-1/2}\right), \\ (hu)_i^{n+1} &= (hu)_i^{n+1-} - \frac{\Delta t}{\Delta x}\left((hu)^{*,n+1-}_{i+1/2} u^{*,n+1-}_{i+1/2} - (hu)^{*,n+1-}_{i-1/2} u^{*,n+1-}_{i-1/2}\right) \\ &\quad + \frac{\Delta t}{\Delta x}\left((hu)_i^{n+1-}\left(u^{e,t_{n+1-}}_{i,i+1/2} - u^{e,t_{n+1-}}_{i,i-1/2}\right)\right), \end{aligned} \tag{3.2}$$

where $u^{e,t_{n+1-}}_{i,i\pm 1/2} = u^{e,t_{n+1-}}_i(x_{i\pm 1/2})$. Note that now, the values $u^{*,n+1-}_{i+1/2}$ and $h^{*,n+1-}_{i\pm 1/2}$ and $(hu)^{*,n+1-}_{i\pm 1/2}$ must be determined. The values $u^{*,n+1-}_{i+1/2}$ are computed at each intercell by means of a fully well-balanced first order reconstruction operator as follows:

$$u^{*,n+1-}_{i+1/2} = \frac{P^{o1}_{i,\overrightarrow{w}}(x_{i+1/2}, t^{n+1-}) - P^{o1}_{i+1,\overrightarrow{w}}(x_{i+1/2}, t^{n+1-})}{2a}.$$

Finally the values $h^{*,n+1-}_{i\pm 1/2}$ and $(hu)^{*,n+1-}_{i\pm 1/2}$ are also computed using again the fully well-balanced first order reconstruction operator and the upwind scheme, that is,

$$X^{*,n+1-}_{i+1/2} = \begin{cases} P^{o1}_{i,X}(x_{i+1/2}) & \text{if} \quad u^{*,n+1-}_{i+1/2} \geq 0, \\ P^{o1}_{i+1,X}(x_{i+1/2}) & \text{if} \quad u^{*,n+1-}_{i+1/2} < 0, \end{cases}$$

where $X = h, hu$.

Note that here we have used a splitting technique by solving first the system defined by S_P and then the one defined by S_T. Nevertheless, nothing obliges one to do the splitting in that order and one could consider a variant of this explicit scheme by solving first (2.6) and then (2.5).

3.2. Semi-implicit scheme. As previously said, in subcritical regimes where $u^2 << gh$, the main restriction of the CFL condition comes from the pressure terms. Therefore, in view of the eigenvalues of (2.5) (see (2.7)) we consider an implicit version of the pressure system:

$$\begin{aligned} &h_i^{n+1-} = h_i^n, \\ &(hu)_i^{n+1-} = (hu)_i^n - \frac{\Delta t}{\Delta x}\left(\pi^{*,n+1-}_{i+1/2} - \pi^{*,n+1-}_{i-1/2} - \pi^{e,n}_i(x_{i+1/2}) + \pi^{e,n}_i(x_{i-1/2})\right). \end{aligned} \tag{3.3}$$

It can be seen that $(hu)_i^{n+1-}$ could be also obtained as

$$(hu)_i^{n+1-} = h_i^n u_i^{n+1-} = h_i^n \cdot \frac{\overrightarrow{w}_i^{n+1-} - \overleftarrow{w}_i^{n+1-}}{2a},$$

where $\overrightarrow{w}_i^{n+1-}$ and $\overleftarrow{w}_i^{n+1-}$ are given by

$$\overrightarrow{w}_i^{n+1-} = \overrightarrow{w}_i^n - \frac{a\Delta t}{h_i^n \Delta x}\left(\overrightarrow{w}^{n+1}_{i+1/2} - \overrightarrow{w}^{n+1}_{i-1/2} - \overrightarrow{w}^{e,n}_{i+1/2} + \overrightarrow{w}^{e,n}_{i-1/2}\right),$$

and

$$\overleftarrow{w}_i^{n+1-} = \overleftarrow{w}_i^n + \frac{a\Delta t}{h_i^n \Delta x}\left(\overleftarrow{w}^{n+1}_{i+1/2} - \overleftarrow{w}^{n+1}_{i-1/2} - \overleftarrow{w}^{e,n}_{i+1/2} + \overleftarrow{w}^{e,n}_{i-1/2}\right),$$

where $\overrightarrow{w}^{n+1}_{i+1/2}$ is given by

$$\begin{aligned} \overrightarrow{w}^{n+1}_{i+1/2} &= P^{o1}_{i,\overrightarrow{w}}(x_{i+1/2}, t^{n+1}) \\ &= \overrightarrow{w}_i^{n+1} - \pi^{e,n}_i(x_i) - a u^{e,n}_i(x_i) + \pi^{e,n}_i(x_{i+1/2}) + a u^{e,n}_i(x_{i+1/2}), \end{aligned}$$

$\overleftarrow{w}^{n+1}_{i+1/2}$ is defined similarly, and

$$\overrightarrow{w}^{e,n}_{i\pm 1/2} = \frac{1}{2} g (h^e_i)^2 (x_{i\pm 1/2}) + a u^e_i(x_{i\pm 1/2}).$$

Therefore, for the pressure step we first solve these systems for $\overrightarrow{w}$ and $\overleftarrow{w}$, which are linear and easy to solve, and we use its solution to compute (3.3). In this work the implicit systems are solved using a direct method.

Next, the transport step is computed as in the explicit case.

As we have said for the explicit case, we may reverse the order of the splitting so that we may first solve system (2.6) and then system (2.5). Of course, system (2.6) would be solved explicitly and (2.5), implicitly.

4. Second order scheme. In order to obtain second order accuracy, the time-stepping will be done using a Strang splitting method (see [47, 40, 41]). More explicitly,

1. perform a step of the first system with time step $\Delta t/2$, obtaining an approximation $\widetilde{h}_i^{n+1}$ and $\widetilde{(hu)}_i^{n+1}$;
2. perform a step of the second system with time step Δt, obtaining the approximation denoted by $\widehat{h}_i^{n+1}$ and $\widehat{(hu)}_i^{n+1}$;
3. perform a final step of the first system with time step $\Delta t/2$, obtaining the approximations h_i^{n+1} and $(hu)_i^{n+1}$ at time t^{n+1}.

Let us remark that there is no a priori restriction on which of the systems (2.5) or (2.6) should go first.

This may be summarized in a compact form as follows:

Denote by S_P^τ, S_T^τ the approximate solution operators in the interval $[t, t+\tau]$ of the corresponding exact solution operators to the pressure system S_P and transport system S_T, respectively. Then, the first version of the scheme corresponds to

$$U(x, t+\Delta t) = S_P^{\frac{\Delta t}{2}} \circ S_T^{\Delta t} \circ S_P^{\frac{\Delta t}{2}}(U(x,t)), \tag{4.1}$$

while the second version corresponds to

$$U(x, t+\Delta t) = S_T^{\frac{\Delta t}{2}} \circ S_P^{\Delta t} \circ S_T^{\frac{\Delta t}{2}}(U(x,t)), \tag{4.2}$$

Note that in each of the steps we need to consider second order approximations in space, while the time stepping is just first order within the step, the second order in time being obtained thanks to the Strang method.

4.1. Explicit scheme. We shall describe the case corresponding to (4.1). The second version given by (4.2) is analogous.

In this explicit case, the solution of the first step is obtained by applying (3.1) with time step $\Delta t/2$. Afterward, we solve the transport system using (3.2), and finally the pressure system is solved again applying (3.1) with time step $\Delta t/2$. Of course, in the previous schemes, second order approximations in space are considered.

4.2. Semi-implicit scheme. As before, we will describe the case corresponding to (4.1). In this case, similarly as done for the first order scheme, the steps corresponding to the operator S_P are performed implicitly. Therefore, we use the same procedure as in the second order explicit case but now using for the pressure system the implicit scheme (3.3) instead of (3.1).

Note that the semi-implicit second order scheme requires solving linear systems for the pressure step. Therefore, accounting for the computational cost, in this case it is especially interesting to consider the second version of the scheme, where only one step corresponds to the pressure system.

5. Numerical experiments. In this section, we consider a wide range of numerical experiments in order to test the performance of the different schemes proposed here. We will denote by EXP the results obtained by the fully explicit schemes and by IMP the semi-implicit ones. The accuracy will be indicated as O1 or O2 for the first or second order, respectively. Moreover, the different versions of the schemes will be denoted by PT, TP, PTP, and TPT, which indicate the order in which the pressure (P) and the transport (T) systems have been solved.

From now on, when we say CFL > 1, we refer to the stability restriction associated to the sound speed. However, our semi-implicit schemes do have a stability restriction due to the projection step (associated to the velocity). So we cannot take the CFL related to the sound speed to be as big as we want, since it is limited by the projection CFL.

Last, unless otherwise stated, the value of g is taken to be 9.8 and periodic boundary conditions are considered.

5.1. Fully well-balanced property. In order to check that the fully well-balanced property is satisfied, we consider the spatial domain $[-5,5]$ and define as bottom topography a Gaussian bump given by

$$z(x) = 0.5\exp(-x^2). \tag{5.1}$$

Then, a subcritical steady state is computed by setting $C_1 = hu = 0.1$ and constant energy level

$$C_2 = \frac{(0.1)^2}{2} + g(1 + z(-5)),$$

which corresponds to the value obtained by imposing $h = 1$ at the left boundary. This subcritical steady state is considered as the initial condition for the schemes, and its mean Froude number is between 0.03 and 0.09.

Tables 1 and 2 show the difference in L^1 norm between the initial condition and the solution obtained with the schemes at time $t = 1$ with $N = 100$ cells in the domain and setting the CFL value to 1 for the explicit schemes and 5 for the implicit ones. As expected, the steady state is preserved, obtaining errors of order 10^{-14}. The mean time step in the explicit case is 0.01, while in the implicit one it is 0.07, which is 7 times bigger.

5.2. Accuracy test. Let us now check the order of the schemes by performing an accuracy test. To do so, we consider as the initial condition a small perturbation of water at a rest steady state:

TABLE 1

Difference in L^1 norm between the initial condition and the solution obtained at time $t = 1$ with each of the first order schemes.

EXP O1 PT		EXP O1 TP		IMP O1 PT		IMP O1 TP	
h	hu	h	hu	h	hu	h	hu
5.83e−14	5.80e−14	4.54e−14	6.57e−14	8.14e−14	9.97e−14	6.82e−14	7.58e−14

TABLE 2

Difference in L^1 norm between the initial condition and the solution obtained at time $t = 1$ with each of the second order schemes.

EXP O2 PTP		EXP O2 TPT		IMP O2 PTP		IMP O2 TPT	
h	hu	h	hu	h	hu	h	hu
4.01e−14	6.87e−14	3.44e−14	5.74e−14	5.41e−14	8.41e−14	4.80e−14	8.13e−14

$$h(x,0)=\begin{cases} 0.05\left(1+\cos\left(\frac{2\pi(x-4750)}{3500}\right)\right) & \text{if} \quad 3000<x<6500,\\ 0.05\left(-\left(1+\cos\left(\frac{2\pi(x-9250)}{3500}\right)\right)\right) & \text{if} \quad 7500<x<11000,\\ 0 & \text{otherwise}\end{cases}$$

with $q(x,0)=0$ and bottom topography

$$z(x)=-\left(50-\exp\left(-\frac{(x-7000)^2}{1000000}\right)\right).$$

The spatial domain corresponds to $[0,14000]$ and the final time is $t=0.5$. Periodic boundary conditions are considered. The considered reference solution has 6400 cells. In this test, the mean Froude number is lower than $9\cdot 10^{-6}$.

The errors are shown in Tables 3, 4, 5, and 6. The expected order is reached for either the explicit or the semi-implicit version. We remark that, concerning the order of convergence, no major differences are observed if we begin with either the pressure or the transport system. Therefore, focusing exclusively in the order of accuracy, it would make sense to start with the transport system for the second order semi-implicit scheme, since the computational cost would be less.

Table 3
Errors in L^1 norm and convergence rates for the first order explicit schemes.

No. of	EXP O1 PT (CFL 1)				EXP O1 TP (CFL 1)			
	h		q		h		q	
cells	Error	Order	Error	Order	Error	Order	Error	Order
100	2.82e+00		1.38e+00		2.82e+00		1.44e+00	
200	7.50e-01	1.91	4.22e-01	1.71	7.50e-01	1.91	4.55e-01	1.66
400	2.28e-01	1.72	1.39e-01	1.60	2.28e-01	1.72	1.56e-01	1.55
800	7.93e-02	1.53	4.91e-02	1.50	7.93e-02	1.53	5.73e-02	1.44
1600	2.91e-02	1.45	1.75e-02	1.49	2.91e-02	1.45	2.12e-02	1.43

Table 4
Errors in L^1 norm and convergence rates for the first order implicit schemes.

No. of	IMP O1 PT (CFL 5)				IMP O1 TP (CFL 5)			
	h		q		h		q	
cells	Error	Order	Error	Order	Error	Order	Error	Order
100	2.82e+00		1.51e+00		2.82e+00		1.57e+00	
200	7.51e-01	1.91	4.89e-01	1.62	7.51e-01	1.91	5.23e-01	1.59
400	2.29e-01	1.71	1.73e-01	1.50	2.29e-01	1.71	1.90e-01	1.46
800	7.98e-02	1.52	6.54e-02	1.40	7.98e-02	1.52	7.32e-02	1.37
1600	2.96e-02	1.43	2.47e-02	1.40	2.96e-02	1.43	2.81e-02	1.38

Table 5
Errors in L^1 norm and convergence rates for the second order explicit schemes.

No. of	EXP O2 PTP (CFL 1)				EXP O2 TPT (CFL 1)			
	h		q		h		q	
cells	Error	Order	Error	Order	Error	Order	Error	Order
100	3.05e+00		2.30e+00		3.05e+00		2.31e+00	
200	7.64e-01	2.00	5.43e-01	2.08	7.64e-01	2.00	5.43e-01	2.09
400	1.91e-01	2.00	1.26e-01	2.11	1.91e-01	2.00	1.25e-01	2.12
800	4.73e-02	2.01	3.09e-02	2.02	4.73e-02	2.01	3.06e-02	2.03
1600	1.13e-02	2.06	7.80e-03	1.99	1.13e-02	2.06	7.97e-03	1.94

TABLE 6
Errors in L^1 norm and convergence rates for the second order implicit schemes.

No. of	IMP O2 PTP (CFL 5)				IMP O2 TPT (CFL 5)			
	h		q		h		q	
cells	Error	Order	Error	Order	Error	Order	Error	Order
100	3.05e+00		2.29e+00		3.05e+00		2.28e+00	
200	7.64e-01	2.00	5.44e-01	2.07	7.64e-01	2.00	5.44e-01	2.07
400	1.91e-01	2.00	1.26e-01	2.11	1.91e-01	2.00	1.26e-01	2.11
800	4.73e-02	2.01	3.10e-02	2.03	4.73e-02	2.01	3.06e-02	2.04
1600	1.13e-02	2.06	7.44e-03	2.06	1.13e-02	2.07	7.26e-03	2.07

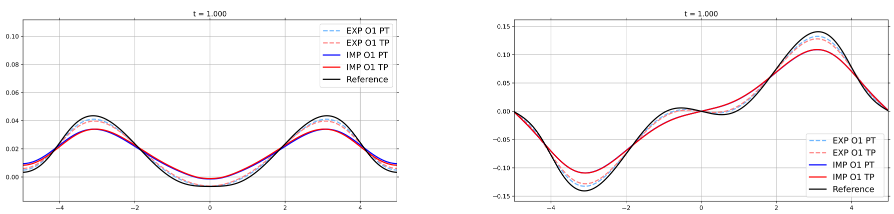

(a) η (b) q

FIG. 1. *Solution at time $t = 1$ obtained with the first order schemes using 200 cells.*

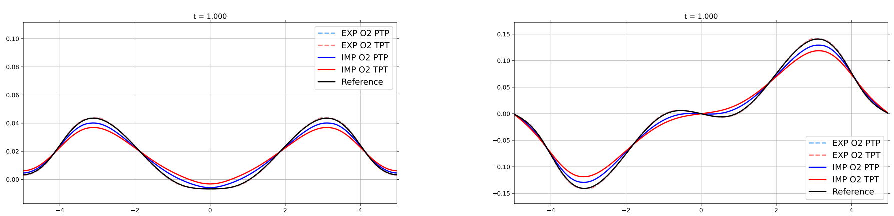

(a) η (b) q

FIG. 2. *Solution at time $t = 1$ obtained with the second order schemes using 200 cells.*

The mean time step has also been computed for the case of 3200 cells, resulting in 0.16 for the explicit case and 0.5 for the implicit one, which is 3 times bigger.

5.3. Perturbation of water at rest. We propose now to closely study the behavior of the different schemes. Let us consider the bottom topography given by (5.1) in the domain $[-5,5]$. The following perturbation of water at rest is considered as the initial condition:

$$h(x) = -z(x) + 0.1e^{-x^2},\ u(x) = 0.$$

In this test the mean Froude number depends on time and varies on $[0, 0.04]$.

In Figures 1 and 2 we can see the solution obtained with the first and second order schemes at time $t = 1$ using 200 cells and CFL 0.8 for the explicit schemes and 2 for the implicit ones. In both figures we have also plotted a reference solution that has been computed using the EXP O1 PT scheme with 1600 cells. Again, periodic boundary conditions have been considered.

As expected, the implicit schemes are more diffusive than the explicit ones. However, this diffuseness is reduced when we consider second order schemes. In this case, the mean time step is 0.006 for the explicit schemes and 0.016 for the implicit ones, which is more than 2.5 times bigger.

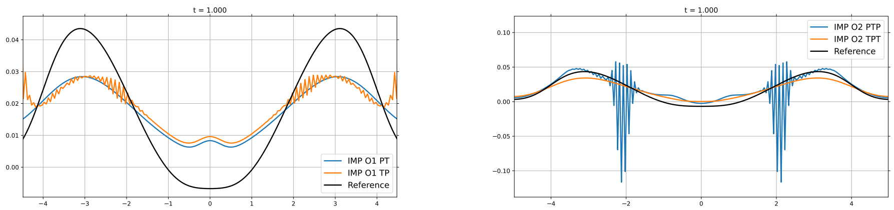

(a) First order schemes (CFL 5) (b) Second order schemes (CFL 3)

FIG. 3. *Solution for η at time $t=1$ obtained using* 200 *cells when increasing the CFL.*

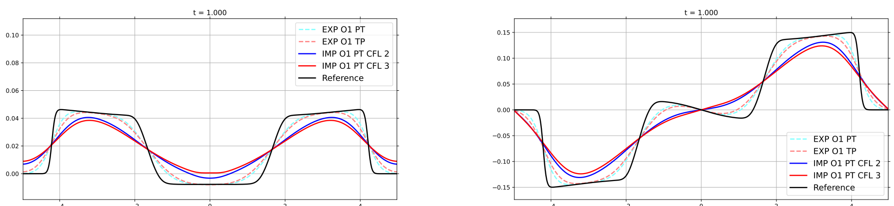

(a) η (b) q

FIG. 4. *Solution at time $t=1$ obtained with the first order schemes using* 200 *cells.*

Let us now consider a bigger CFL number for the implicit schemes, which is shown in Figure 3. We now note a major difference whether we begin with the pressure or the transport system. As shown on the left-hand side in Figure 3, with CFL $=5$, the IMP O1 PT scheme performs better in terms of stability than the IMP O1 TP. Conversely, on the right-hand side for the second order case, the IMP O2 TPT scheme shows better performance than the IMP O2 PTP in terms of stability. Therefore, from now on, we will just consider the IMP O1 PT and IMP O2 TPT versions of the semi-implicit schemes.

5.4. Perturbation of water at rest with shock waves. Up to this point, the numerical tests considered corresponded to smooth solutions. We want now to check the performance of the schemes in the presence of shocks. In order to do so we consider the same bottom topography as in the previous test case, that is, the topography given by (5.1), and define the following initial condition in $[-5,5]$:

$$h(x)=\begin{cases} -z(x) & \text{if} \quad |x|\geq 1, \\ -z(x)+0.1 & \text{if} \quad |x|<1, \end{cases} \qquad u(x)=0.$$

Periodic boundary conditions will be used. The mean Froude number here is lower than 0.06.

Figures 4 and 5 show the solutions obtained at time $t=1$ for the first and second order schemes, respectively. For the explicit schemes the CFL value has been set to 0.8 and for the implicit ones we have considered two cases: solution with CFL 2 and with CFL 3. In order to compare the results, we include the reference solution computed with the EXP O1 PT scheme and 1600 cells.

We have also computed the mean time step, obtaining 0.006 for the explicit schemes and, in the implicit case, 0.016 for CFL 2 and 0.025 for CFL 3.

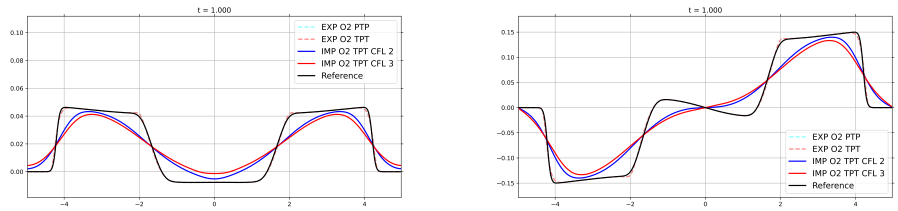

(a) η (b) q

Fig. 5. *Solution at time $t = 1$ obtained with the second order schemes using 200 cells.*

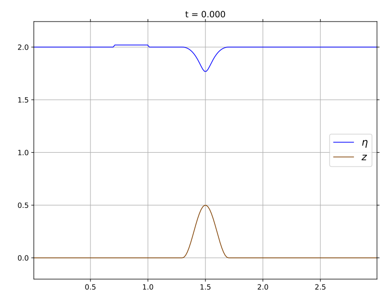

Fig. 6. *Perturbation of a subcritical solution initial condition.*

We observe that the schemes successfully handle the initial condition, not observing important spurious oscillations for the second order schemes. This might be thanks to the use of slope limiters in the reconstruction operators.

5.5. Perturbation of a subcritical solution. We will now perform a test proposed in [34], in which a perturbation of a smooth subcritical stationary solution is considered as the initial condition. The initial condition will be given by $U_0(x) = (h_0(x), q_0(x))^t$ for $x \in [0, 3]$, where

$$h_0(x) = \begin{cases} h^*(x) + 0.02 & \text{if} \quad 0.7 \leq x \leq 1, \\ h^*(x) & \text{otherwise,} \end{cases}$$

and $q_0(x) = q^*(x)$, where $U^*(x) = (h^*(x), q^*(x))^t$, the solution of the following Cauchy problem (1.2) with initial condition $h(0) = 2, q(0) = 3.5$. Moreover, the bottom topography is given by

$$z(x) = \begin{cases} 0.25(1 + \cos(5\pi(x + 0.5))) & \text{if} \quad 1.3 \leq x \leq 1.7, \\ 0 & \text{otherwise.} \end{cases} \tag{5.2}$$

This initial condition has been plotted in Figure 6.

As boundary conditions, we impose the value of q on the left and the one of h on the right and the gravity constant is set to be $g = 9.812$. In this case, the mean Froude number is between 0.38 and 0.78.

In Figure 7 we have plotted the difference between the result of the scheme and the steady state at time $t = 0.1$ using $N = 200$ cells for the first and second order schemes for the variable h. A reference solution has been computed using the first order explicit scheme with 1600 cells. For the implicit schemes, the CFL value has been set to 5. The mean time step is 0.002 for the explicit schemes and 0.005 for the implicit ones.

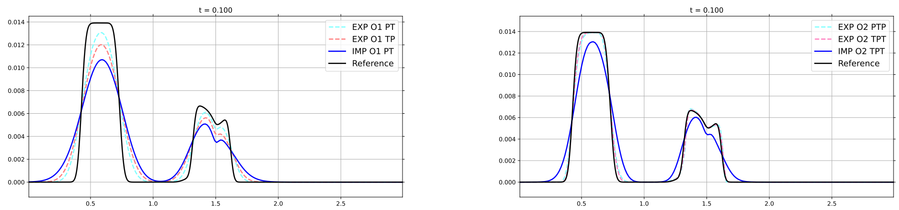

(a) First order schemes (b) Second order schemes

FIG. 7. *Difference between the result of the scheme and the steady state at time* $t = 0.1$ *using* $N = 200$ *cells for the variable* h*.*

TABLE 7
Error in L^1 *norm and CPU time for the different schemes at time* $t = 10$ *using* 100 *cells.*

Scheme	Error for h	CPU time
EXP O1 PT	$1.31 \cdot 10^{-3}$	40.79
EXP O1 TP	$1.12 \cdot 10^{-3}$	41.29
IMP O1 PT	$7.75 \cdot 10^{-4}$	45.47
EXP O2 PTP	$1.62 \cdot 10^{-3}$	126.82
EXP O2 TPT	$1.64 \cdot 10^{-3}$	129.70
IMP O2 TPT	$1.22 \cdot 10^{-3}$	96.62

TABLE 8
Error in L^1 *norm and CPU time for the different schemes at time* $t = 100$ *using* 100 *cells.*

Scheme	Error for h
EXP O1 PT	$3.94 \cdot 10^{-13}$
EXP O1 TP	$3.73 \cdot 10^{-13}$
IMP O1 PT	$2.86 \cdot 10^{-13}$
EXP O2 PTP	$3.86 \cdot 10^{-13}$
EXP O2 TPT	$2.14 \cdot 10^{-13}$
IMP O2 TPT	$2.93 \cdot 10^{-13}$

We clearly observe the well-balanced character of the schemes, since they preserve the stationary solution in the areas where the perturbation has not arrived yet.

Moreover, in Table 7, we show the errors for h and the CPU times at time $t = 10$ for the different schemes using 100 cells. In the first order case, the semi-implicit scheme takes some more seconds than the explicit one but the error is also lower than the others. However, in the second order case we observe errors of the same magnitude and the CPU time needed by the semi-implicit scheme is approximately 25% lower than the explicit ones. Of course, if we increase the final time and the perturbation leaves the domain, we capture the steady state, as shown in Table 8.

5.6. Perturbation of a transcritical smooth solution. For this test, we will once again take into account a test proposed in [19] consisting in a stationary solution with a transition at $x_{crit} = 1.5$ which is the solution of (1.2) with constants $C_1 = 2.5$ and $C_2 = 17.56957396120237$, and the same depth function as in previous tests, (5.2). A small perturbation of size $\Delta h = 0.02$ is imposed in the interval $[1.1, 1.2]$. This initial condition is plotted in Figure 8. As boundary conditions, we impose the value of q on the left and leave free boundary conditions on the right and, as in the previous test, the gravity constant is set to be $g = 9.812$. Now, the mean Froude number is between 0.36 and 2.28.

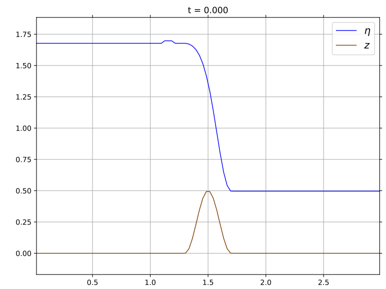

FIG. 8. *Perturbation of a transcritical smooth solution initial condition.*

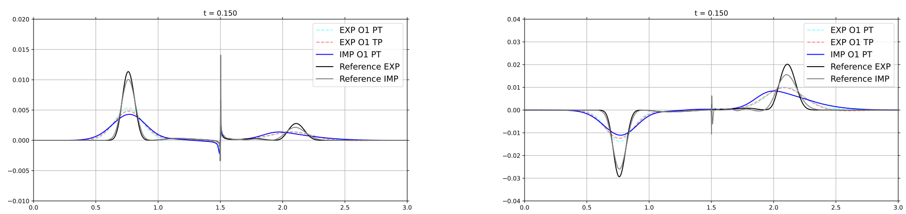

(a) h

(b) q

FIG. 9. *Difference between the result of the first order schemes and the steady state at time* $t = 0.15$ *using* 200 *cells.*

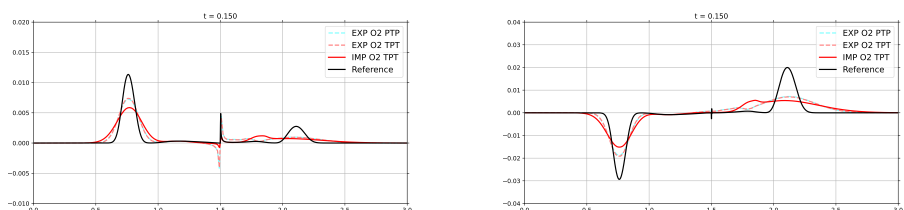

(a) h

(b) q

FIG. 10. *Difference between the result of the second order schemes and the steady state at time* $t = 0.15$ *using* 200 *cells.*

In Figures 9 and 10, we have plotted the difference between the result of the different schemes and the steady state at time $t = 0.15$ using 200 cells and CFL 1.36 for the implicit schemes, which is the maximum CFL that the transport step restriction allows us to set. Again, the reference solution has been computed by using the first order explicit scheme with 1600 cells. In this test, we do not see big differences in the mean time step between the explicit and the implicit schemes, since the CFL of the implicit schemes cannot be taken to be too big.

It might look like in the implicit case the right wave is shifted to the left with respect to the reference solution, but this is due to diffusion. To be sure about this, for the first order case we have also computed a reference solution with the implicit scheme by increasing the number of cells to 1600 and setting the CFL value to be 1, observing that the solutions converge to a reference solution computed with the explicit scheme. Moreover, the peak of the sonic point is not as pronounced as it appears to be. In order to show this we have plotted the free surface for the different

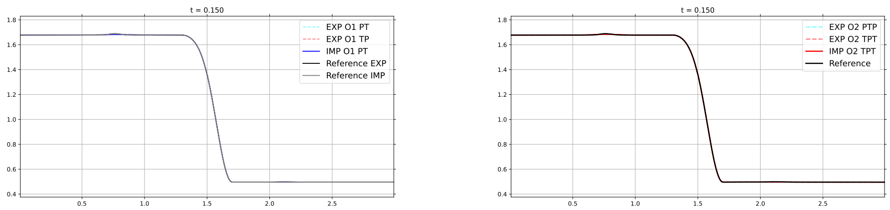

(a) First order schemes (b) Second order schemes

FIG. 11. *Solution for the free surface at time* $t = 0.15$ *obtained using* 200 *cells.*

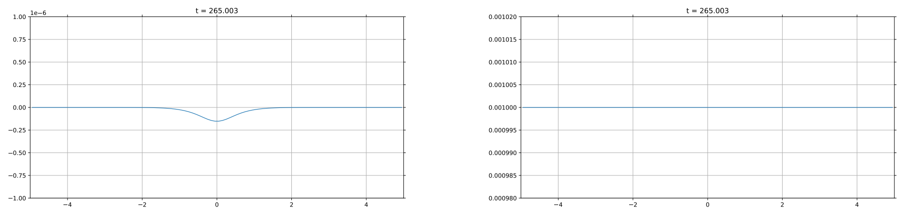

(a) η (b) q

FIG. 12. *Subcritical solution obtained after convergence.*

schemes in Figure 11, where no big differences are observed between the different schemes.

5.7. Convergence to a subcritical steady state. Let us consider again the bottom topography (5.1) and a water at rest initial condition in the interval $[-5,5]$:

$$\eta = h + z = 0, \quad u = 0.$$

At the left boundary, we impose a discharge given by $q(x=-5,t) = 0.001$ and at the right boundary we fix the water height to $h(x=5,t)=1$, using a ghost-cell technique and 100 cells. We set the CFL to be the maximum value allowed by the transport restriction for the semi-implicit schemes, which in this case is 62, and let the scheme run until the difference in L^1 norm between one iteration at the next one is less than 10^{-12}. When that happens, the solution should have converged to a subcritical stationary steady state. In this test, the mean Froude number is of order 10^{-4}.

Here we show the results obtained for the first order implicit scheme, and the second order implicit scheme should give similar results.

In this case, the convergence restriction was achieved at time $t = 265.003$, with the mean time step considered being 0.9925. Moreover, the CPU time needed was 11.25 seconds. Last, we have also checked that, indeed, the discharge and the energy of the solution obtained are constant. In fact, the errors are of order 10^{-12}. In Figure 12 we plot the free surface and the discharged obtained at the final time.

6. Conclusions. We have designed first and second order schemes for the shallow water equations by applying a splitting technique that allows us to separate the acoustic and the transport waves. This gives us a pressure system and a transport one. Even though the transport system is always solved explicitly, the fact that the pressure one is solved implicitly allows us to consider a less restrictive CFL condition and bigger time steps. In order to easily solve the pressure system, a relaxation technique has been applied. In the numerical tests we have seen a reduction in the computational time required by the implicit schemes with respect to the explicit ones in low Froude number situations. Moreover, we have verified that our schemes are fully well-balanced, so they are able to preserve all the steady states of the shallow water equations.

This strategy could be applied to other models such as the Ripa model or a two-layer model that could benefit from this splitting. Moreover, one could also consider applying this strategy to two-dimensional models.

REFERENCES

[1] E. Audusse, F. Bouchut, M. O. Bristeau, R. Klein, and B. Perthame, *A fast and stable well-balanced scheme with hydrostatic reconstruction for shallow water flows*, SIAM J. Sci. Comput., 25 (2004), pp. 2050–2065, https://doi.org/10.1137/S1064827503431090.

[2] E. Audusse, C. Chalons, and P. Ung, *A simple well-balanced and positive numerical scheme for the shallow-water system*, Commun. Math. Sci., 13 (2015), pp. 1317–1332, https://doi.org/10.4310/CMS.2015.v13.n5.a11.

[3] M. Baudin, C. Berthon, F. Coquel, R. Masson, and Q. H. Tran, *A relaxation method for two-phase flow models with hydrodynamic closure law*, Numer. Math., 99 (2004), pp. 411–440, https://doi.org/10.1007/s00211-004-0558-1.

[4] A. Bermudez and M. E. Vazquez, *Upwind methods for hyperbolic conservation laws with source terms*, Comput. & Fluids, 23 (1994), pp. 1049–1071, https://doi.org/10.1016/0045-7930(94)90004-3.

[5] C. Berthon and C. Chalons, *A fully well-balanced, positive and entropy-satisfying Godunov-type method for the shallow-water equations*, Math. Comp., 85 (2015), pp. 1281–1307, https://doi.org/10.1090/mcom3045.

[6] C. Berthon, C. Chalons, S. Cornet, and G. Sperone, *Fully well-balanced, positive and simple approximate Riemann solver for shallow water equations*, Bull. Braz. Math. Soc. (N.S.), 47 (2016), pp. 117–130, https://doi.org/10.1007/s00574-016-0126-1.

[7] C. Berthon and F. Foucher, *Efficient well-balanced hydrostatic upwind schemes for shallow-water equations*, J. Comput. Phys., 231 (2012), pp. 4993–5015, https://doi.org/10.1016/j.jcp.2012.02.031.

[8] C. Berthon and V. Michel-Dansac, *A simple fully well-balanced and entropy preserving scheme for the shallow-water equations*, Appl. Math. Lett., 86 (2018), pp. 284–290, https://doi.org/10.1016/j.aml.2018.07.013.

[9] G. Bispen, K. R. Arun, M. Lukáčová-Medvid'ová, and S. Noelle, *IMEX large time step finite volume methods for low Froude number shallow water flows*, Commun. Comput. Phys., 16 (2014), pp. 307–347, https://doi.org/10.4208/cicp.040413.160114a.

[10] L. Bonaventura, E. D. Fernández-Nieto, J. Garres-Díaz, and G. Narbona-Reina, *Multilayer shallow water models with locally variable number of layers and semi-implicit time discretization*, J. Comput. Phys., 364 (2018), pp. 209–234, https://doi.org/10.1016/j.jcp.2018.03.017.

[11] W. Boscheri, M. Tavelli, and C. E. Castro, *An all Froude high order IMEX scheme for the shallow water equations on unstructured Voronoi meshes*, Appl. Numer. Math., 185 (2023), pp. 311–335, https://doi.org/10.1016/j.apnum.2022.11.022.

[12] F. Bouchut, *Entropy satisfying flux vector splittings and kinetic BGK models*, Numer. Math., 94 (2003), pp. 623–672, https://doi.org/10.1007/s00211-002-0426-9.

[13] F. Bouchut, *Nonlinear Stability of Finite Volume Methods for Hyperbolic Conservation Laws and Well-balanced Schemes for Sources*, Front. Math., Birkhäuser Verlag, Basel, 2004.

[14] F. Bouchut, E. Franck, and L. Navoret, *A low cost semi-implicit low-Mach relaxation scheme for the full Euler equations*, J. Sci. Comput., 83 (2020), https://doi.org/10.1007/s10915-020-01206-z.

[15] F. Bouchut and T. Morales de Luna, *A subsonic-well-balanced reconstruction scheme for shallow water flows*, SIAM J. Numer. Anal., 48 (2010), pp. 1733–1758, https://doi.org/10.1137/090758416.

[16] S. Busto and M. Dumbser, *A staggered semi-implicit hybrid finite volume/ finite element scheme for the shallow water equations at all Froude numbers*, Appl. Numer. Math., 175 (2022), pp. 108–132, https://doi.org/10.1016/j.apnum.2022.02.005.

[17] C. Caballero-Cárdenas, M. J. Castro, T. Morales de Luna, and M. L. Muñoz-Ruiz, *Implicit and implicit-explicit Lagrange-projection finite volume schemes exactly well-balanced for 1D shallow water system*, Appl. Math. Comput., 443 (2023), 127784, https://doi.org/10.1016/j.amc.2022.127784.

[18] M. J. Castro, C. Chalons, and T. Morales de Luna, *A fully well-balanced Lagrange–projection-type scheme for the shallow-water equations*, SIAM J. Numer. Anal., 56 (2018), pp. 3071–3098, https://doi.org/10.1137/17m1156101.

[19] M. J. Castro, J. A. López-García, and C. Parés, *High order exactly well-balanced numerical methods for shallow water systems*, J. Comput. Phys., 246 (2013), pp. 242–264, https://doi.org/10.1016/j.jcp.2013.03.033.

[20] M. J. Castro and C. Parés, *Well-balanced high-order finite volume methods for systems of balance laws*, J. Sci. Comput., 82 (2020), https://doi.org/10.1007/s10915-020-01149-5.

[21] V. Casulli, *Semi-implicit finite difference methods for the two-dimensional shallow water equations*, J. Comput. Phys., 86 (1990), pp. 56–74, https://doi.org/10.1016/0021-9991(90)90091-E.

[22] V. Casulli and R. T. Cheng, *Semi-implicit finite difference methods for three-dimensional shallow water flow*, Internat. J. Numer. Methods Fluids, 15 (1992), pp. 629–648, https://doi.org/10.1002/fld.1650150602.

[23] L. Cea and A. López-Núñez, *Extension of the two-component pressure approach for modeling mixed free-surface-pressurized flows with the two-dimensional shallow water equations*, Internat. J. Numer. Methods Fluids, 93 (2020), pp. 628–652, https://doi.org/10.1002/fld.4902.

[24] C. Chalons, Thesis "Bilans d'entropie discrets dans l'approximation numérique des chocs non classiques. application aux équations de navier-stokes multi-pression 2d et à quelques systèmes visco-capillaires", École Polytechnique Palaiseau, France, 2002.

[25] C. Chalons, M. Girardin, and S. Kokh, *An All-Regime Lagrange-Projection Like Scheme for the Gas Dynamics Equations on Unstructured Meshes*, Commun. Comput. Phys., 20 (2016), pp. 188–233, https://doi.org/10.4208/cicp.260614.061115a.

[26] A. Chinnayya, A.-Y. Leroux, and N. Seguin, *A well-balanced numerical scheme for the approximation of the shallow-water equations with topography: The resonance phenomenon*, Int. J. Finite Vol., 1 (2004).

[27] F. Coquel, E. Godlewski, B. Perthame, A. In, and P. Rascle, *Some new Godunov and relaxation methods for two-phase flow problems*, in Godunov Methods, Springer, New York, 2001, pp. 179–188, https://doi.org/10.1007/978-1-4615-0663-8_18.

[28] M. Dumbser and V. Casulli, *A staggered semi-implicit spectral discontinuous Galerkin scheme for the shallow water equations*, Appl. Math. Comput., 219 (2013), pp. 8057–8077.

[29] E. Franck and L. Navoret, *Semi-implicit two-speed well-balanced relaxation scheme for Ripa model*, in Springer Proc. Math. Stat. 323, Springer, New York, 2020, pp. 735–743, https://doi.org/10.1007/978-3-030-43651-3_70.

[30] G. Gallice, *Positive and entropy stable Godunov-type schemes for gas dynamics and MHD equations in Lagrangian or Eulerian coordinates*, Numer. Math., 94 (2002), pp. 673–713, https://doi.org/10.1007/s00211-002-0430-0.

[31] G. Gallice, *Solveurs simples positifs et entropiques pour les systèmes hyperboliques avec terme source*, C. R. Math., 334 (2002), pp. 713–716, https://doi.org/10.1016/S1631-073X(02)02307-5.

[32] J.-F. Gerbeau and B. Perthame, *Derivation of viscous Saint-Venant system for laminar shallow water; Numerical validation*, Discrete Contin. Dyn. Syst. - B, 1 (2001), pp. 89–102, https://doi.org/10.3934/dcdsb.2001.1.89.

[33] F. X. Giraldo and M. Restelli, *High-order semi-implicit time-integrators for a triangular discontinuous Galerkin oceanic shallow water model*, Internat. J. Numer. Methods Fluids, 63 (2010), pp. 1077–1102, https://doi.org/10.1002/fld.2118.

[34] I. Gómez-Bueno, M. J. Castro, C. Parés, and G. Russo, *Collocation methods for high-order well-balanced methods for systems of balance laws*, Mathematics, 9 (2021), 1799, https://doi.org/10.3390/math9151799.

[35] L. Gosse, *A well-balanced flux-vector splitting scheme designed for hyperbolic systems of conservation laws with source terms*, Comput. Math. Appl., 39 (2000), pp. 135–159, https://doi.org/10.1016/s0898-1221(00)00093-6.

[36] J. M. Greenberg and A. Y. Leroux, *A well-balanced scheme for the numerical processing of source terms in hyperbolic equations*, SIAM J. Numer. Anal., 33 (1996), pp. 1–16, https://doi.org/10.1137/0733001.

[37] D. Iampietro, F. Daude, P. Galon, and J.-M. Hérard, *A Mach-sensitive implicit–explicit scheme adapted to compressible multi-scale flows*, J. Comput. Appl. Math., 340 (2018), pp. 122–150, https://doi.org/10.1016/j.cam.2018.02.019.

[38] S. Jin and Z. Xin, *The relaxation schemes for systems of conservation laws in arbitrary space dimensions*, Comm. Pure Appl. Math., 48 (1995), pp. 235–276, https://doi.org/10.1002/cpa.3160480303.

[39] S. Kang, F. X. Giraldo, and T. Bui-Thanh, *IMEX HDG-DG: A coupled implicit hybridized discontinuous Galerkin and explicit discontinuous Galerkin approach for shallow water systems*, J. Comput. Phys., 401 (2020), 109010, https://doi.org/10.1016/j.jcp.2019.109010.

[40] G. I. Marchuk, *Metody Rasshchepleniya*, Nauka, Moskva, 1988.

[41] G. I. Marchuk, *Splitting and alternating direction methods*, (1990), pp. 197–462, https://doi.org/10.1016/S1570-8659(05)80035-3.

[42] A. Marquina and S. Serna, *Shock-Capturing schemes: High accuracy versus total-variation boundedness*, PAMM, 7 (2007), pp. 1024101–1024102, https://doi.org/10.1002/pamm.200700672.

[43] T. Morales de Luna, M. J. Castro, and C. Chalons, *High-order fully well-balanced Lagrange-projection scheme for shallow water*, Commun. Math. Sci., 18 (2020), pp. 781–807, https://doi.org/10.4310/CMS.2020.v18.n3.a9.

[44] S. Noelle, Y. Xing, and C.-W. Shu, *High-order well-balanced finite volume WENO schemes for shallow water equation with moving water*, J. Comput. Phys., 226 (2007), pp. 29–58, https://doi.org/10.1016/j.jcp.2007.03.031.

[45] B. Perthame and C. Simeoni, *A kinetic scheme for the Saint-Venant system with a source term*, Calcolo, 38 (2001), pp. 201–231, https://doi.org/10.1007/s10092-001-8181-3.

[46] G. Russo and A. Khe, *High order well-balanced schemes based on numerical reconstruction of the equilibrium variables*, in Waves and Stability in Continuous Media, World Scientific, Englewod Cliffs, NJ, 2010, pp. 230–241, https://doi.org/10.1142/9789814317429_0032.

[47] G. Strang, *On the construction and comparison of difference schemes*, SIAM J. Numer. Anal., 5 (1968), pp. 506–517, https://doi.org/10.1137/0705041.

[48] M. Tavelli and M. Dumbser, *A high order semi-implicit discontinuous Galerkin method for the two dimensional shallow water equations on staggered unstructured meshes*, Appl. Math. Comput., 234 (2014), pp. 623–644, https://doi.org/10.1016/j.amc.2014.02.032.

[49] A. Thomann, G. Puppo, and C. Klingenberg, *An all speed second order well-balanced IMEX relaxation scheme for the Euler equations with gravity*, J. Comput. Phys., 420 (2020), 109723, https://doi.org/10.1016/j.jcp.2020.109723.

[50] G. Tumolo, L. Bonaventura, and M. Restelli, *A semi-implicit, semi-Lagrangian, p-adaptive discontinuous Galerkin method for the shallow water equations*, J. Comput. Phys., 232 (2013), pp. 46–67, https://doi.org/10.1016/j.jcp.2012.06.006.

[51] S. Vater and R. Klein, *A semi-implicit multiscale scheme for shallow water flows at low Froude number*, Commun. Appl. Math. Comput. Sci., 13 (2018), pp. 303–336, https://doi.org/10.2140/camcos.2018.13.303.

[52] Y. Xing, *Exactly well-balanced discontinuous Galerkin methods for the shallow water equations with moving water equilibrium*, J. Comput. Phys., 257 (2014), pp. 536–553, https://doi.org/10.1016/j.jcp.2013.10.010.

[53] Y. Xing, C.-W. Shu, and S. Noelle, *On the advantage of well-balanced schemes for moving-water equilibria of the shallow water equations*, J. Sci. Comput., 48 (2010), pp. 339–349, https://doi.org/10.1007/s10915-010-9377-y.